

# Long Range Surface Plasmons in Multilayer Structures

Aida Delfan<sup>1,\*</sup> and J. E. Sipe<sup>1</sup>

<sup>1</sup>*Department of Physics and Institute for Optical Sciences,  
University of Toronto, 60 St. George Street, Ontario M5S 1A7, Canada*

We present a new strategy, based on a Fresnel coefficient pole analysis, for designing an asymmetric multilayer structure that supports long range surface plasmons (LRSP). We find that the electric field intensity in the metal layer of a multilayer LRSP structure can be even slightly smaller than in the metal layer of the corresponding symmetric LRSP structure, minimizing absorption losses and resulting in LRSP propagation lengths up to  $2mm$ . With a view towards biosensing applications, we also present semi-analytic expressions for a standard surface sensing parameter in arbitrary planar resonant structures, and in particular show that for an asymmetric structure consisting of a gold film deposited on a multilayer of  $\text{SiO}_2$  and  $\text{TiO}_2$  a surface sensing parameter  $G = 1.28nm^{-1}$  can be achieved.

## I. INTRODUCTION

Surface plasmon polaritons (or “surface plasmons” (SP) for short) are excitations at metal-dielectric interfaces involving both electronic and electromagnetic degrees of freedom [1]. They have attracted interest for a wide range of applications, including waveguiding and biosensing [2–4], despite the fact that absorption in the metal typically restricts their propagation length to only a few tens of microns. These losses can be minimized if a thin metal layer is situated between two media – a cladding above and a substrate below – with the same dielectric constant. In this symmetric structure the SPs at the two metal-dielectric interfaces can couple and form an excitation in which most of the energy is in the bounding dielectrics, resulting in small propagation losses and propagation lengths of the order of a few millimeters. For this reason, these excitations are called long range surface plasmons (LRSP)[5, 6]. They can survive if the cladding and substrate dielectric constants are not identical, as long as the difference is not too great.

When the cladding above the metal film is a gas or liquid, as in biosensing applications, it is challenging to find a solid substrate that comes close to matching the cladding dielectric constant. If the cladding is an aqueous solution, Teflon and Cytosol are two of the few candidate materials that can provide such a match [7, 8]. An alternate approach is to design an asymmetric layered structure that can support LRSP; examples include a suspended waveguide structure [9] and 1D photonic crystal structures [10, 11]. In this paper, we present a new approach to the design of asymmetric structures for LRSPs, based on a Fresnel coefficient pole analysis. Motivated by biosensing applications, we consider a water cladding, and focus on minimizing the electric field in the metal in order to reduce the losses. In a scenario where the structure is used for sensing the presence of a layer of molecules adsorbed onto the metal film from the water, we calculate the value of a standard surface

sensing parameter [4, 9] that results, and show that in the limit of thin molecular layers it can be derived from a semi-analytic expression that also follows from the pole analysis.

The organization of this paper is as follows: In Sec. II we present our approach for designing a periodic multilayer structure supporting LRSPs. In Sec. III we compare the field intensity profile of the LRSP supported by the multilayer structure to the LRSP in a symmetric structure, and calculate absorption and coupling losses for finite symmetric and asymmetric structures. In Sec. IV we derive a semi-analytic expression for a standard sensing parameter used to characterize the effect of thin molecular layers on the optical properties of arbitrary planar resonant structures, and compare exact and approximate calculations for the structures studied in Sec. III. The paper ends with our conclusions and a comparison with related work.

## II. ASYMMETRIC MULTILAYER STRUCTURES FOR LRSPS

As a reference we begin by considering a symmetric structure, consisting of a thin layer of metal of thickness  $d_m$  with a dielectric constant  $\varepsilon_m$ , sandwiched between a cladding and substrate of the same dielectric constant  $\varepsilon_1$  (Fig. 1a). The Fresnel reflection coefficient for light incident on the metal from the cladding, with wavevector component  $\kappa$  parallel to the interfaces, is

$$R_{cs} = r_{1m} + \frac{t_{1m}r_{m1}t_{m1}e^{2iw_md_m}}{1 - r_{m1}r_{m1}e^{2iw_md_m}}, \quad (1)$$

where  $w_i = \sqrt{\tilde{\omega}^2\varepsilon_i - \kappa^2}$  and  $\tilde{\omega} = \omega/c$  [12]. For real  $\kappa$  we define the square root according to  $\text{Im}\sqrt{Z} \geq 0$ , with  $\text{Re}\sqrt{Z} \geq 0$  if  $\text{Im}\sqrt{Z} = 0$ ; this guarantees that in the limit  $z \rightarrow \pm\infty$  the reflected and transmitted fields, following respectively from Eq. (1) and the corresponding transmission coefficient, are either evanescent moving away from the structure, or carry energy away from it. The  $r_{ij}$  and  $t_{ij}$  are respectively the Fresnel reflection and transmission coefficients from medium  $i$ , with dielectric

\* Corresponding author: adelfan@physics.utoronto.ca

constant  $\varepsilon_i$ , to medium  $j$ , with dielectric constant  $\varepsilon_j$ . For  $s$ -polarized light the coefficients are

$$\begin{aligned} r_{ij} &= \frac{w_i - w_j}{w_i + w_j}, \\ t_{ij} &= \frac{2w_i}{w_i + w_j}, \end{aligned} \quad (2)$$

and for  $p$ -polarized light they are

$$\begin{aligned} r_{ij} &= \frac{w_i \varepsilon_j - w_j \varepsilon_i}{w_i \varepsilon_j + w_j \varepsilon_i}, \\ t_{ij} &= \frac{2n_i n_j w_i}{w_i \varepsilon_j + w_j \varepsilon_i}, \end{aligned} \quad (3)$$

where  $n_i \equiv \sqrt{\varepsilon_i}$ .

Surface electromagnetic resonances are generally signalled by poles in the Fresnel coefficients, indicating that fields can exist near the surface in the absence of incident light. Thus the condition for the LRSP excitation is

$$1 - r_{m1} r_{m1} e^{2i w_m d_m} = 0. \quad (4)$$

For  $p$ -polarized light this can be satisfied at a resonance wavenumber  $\kappa_{res}^{sym}$ , which is complex due to absorption in the metal. The real part of  $\kappa_{res}^{sym}$  is greater than  $\tilde{\omega} n_1$ , indicating a field structure bound to the region of the thin film. We note that the extension of  $\kappa$  from the real axis to the complex plane can introduce subtleties associated with the definition of the square root in  $w_i(\kappa)$ ; we will turn to those in Sec. III, but they will not affect the discussion in this section.

As an example of a symmetric structure we consider a gold metal layer with a thickness  $d_m = 20nm$ , with water as the cladding and substrate. At a wavelength of  $\lambda = 1310nm$ , and with dielectric constants of water and gold taken as  $\varepsilon_{water} = (1.3159 + i1.639 \times 10^{-5})^2$  [9] and  $\varepsilon_{gold} = -86.08 + i8.322$  [9], a numerical search of  $\kappa$  in the complex plane identifies the LRSP by finding the complex value  $\kappa_{res}^{sym}$  where (4) is satisfied for  $p$ -polarized light; we find an effective index for the LRSP of  $n_{eff}^{sym} = 1.31829 + i5.34 \times 10^{-5}$ , where  $n_{eff}^{sym} = \kappa_{res}^{sym} / \tilde{\omega}$ . The very small imaginary part leads to a mode loss of about 2.23dB/mm (also considered by Min et al. [9]), or equivalently an energy propagation length of about 1.95mm.

For any typical LRSP symmetric structure, such as the one above, we suppose that  $\kappa_{res}^{sym}$  has been found. We now want to design an asymmetric structure (Fig. 1b), where the substrate has been replaced by a multilayer, to support LRSPs that mimic those of Fig. 1a. Any surface electromagnetic resonances in this new structure are signalled by poles in the Fresnel coefficients, for example in the reflection coefficient for light incident from the cladding,  $\bar{R}_{1s}$ ,

$$\bar{R}_{1s} = r_{1m} + \frac{t_{1m} \bar{R}_{ms} t_{m1} e^{2i w_m d_m}}{1 - r_{m1} \bar{R}_{ms} e^{2i w_m d_m}}, \quad (5)$$

where  $\bar{R}_{ms}$  is the Fresnel reflection coefficient for light incident from a semi-infinite metal placed above the multilayer structure of interest in Fig. 1b. The reflection

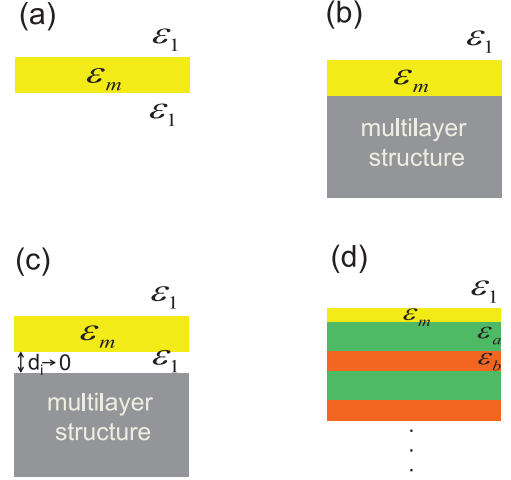


FIG. 1. (a) A symmetric structure for LRSP, with a metal layer between two media with the same dielectric constant, (b) An asymmetric structure with a multilayer substrate beneath the metal layer, (c) an infinitesimally thin layer of medium with dielectric constant  $\varepsilon_1$  inserted under the metal layer, and (d) an asymmetric structure with a metal film supported by an infinite periodic structure consisting of layers of dielectric constant  $\varepsilon_a$  and  $\varepsilon_b$ .

coefficient,  $\bar{R}_{1s}$ , has a pole when

$$1 - r_{m1} \bar{R}_{ms} e^{2i w_m d_m} = 0. \quad (6)$$

This will clearly lead to a  $\kappa_{res}$  equal to  $\kappa_{res}^{sym}$  (recall Eq. (4)), if

$$\bar{R}_{ms} = r_{m1}, \quad (7)$$

where the Fresnel coefficients are evaluated at  $\kappa_{res}^{sym}$ ; we take this as our design target. We can simplify it so that it only involves the properties of the metal layer through a dependence on  $\kappa_{res}^{sym}$  by the following strategy: Insert an infinitesimally thin layer, with a thickness of  $d_i \rightarrow 0$  and dielectric constant  $\varepsilon_1$ , between the metal layer and the multilayer (Fig. 1c). Then  $\bar{R}_{ms}$  is easily found to be

$$\bar{R}_{ms} = r_{m1} + \frac{t_{m1} \mathcal{R}_{1s} t_{1m}}{1 - r_{1m} \mathcal{R}_{1s}}, \quad (8)$$

where  $\mathcal{R}_{1s}$  is the Fresnel reflection coefficient for light incident from the cladding to the multilayer structure, when there is no metal layer present. From Eq. (8), it is clear that (7) is satisfied if  $\mathcal{R}_{1s} = 0$  at  $\kappa_{res}^{sym}$ .

We now specialize to a periodic multilayer structure consisting of layers  $a$  and  $b$ , with respectively thicknesses  $d_a$  and  $d_b$  and real dielectric constants  $\varepsilon_a$  and  $\varepsilon_b$ . For an infinite periodic structure, the Fresnel coefficient  $\mathcal{R}_{1s}$  is given by

$$\begin{aligned} \mathcal{R}_{1s} &= r_{1a} + \frac{t_{1a} R_{per} t_{a1}}{1 - r_{a1} R_{per}}, \\ &= \frac{R_{per} - r_{a1}}{1 - r_{a1} R_{per}}, \end{aligned} \quad (9)$$

where we have assumed the top layer is of type  $a$ , and  $R_{per}$  is the reflection coefficient for light incident on the periodic structure from a semi-infinite medium of dielectric constant  $\varepsilon_a$  (see Fig. 1d). In the second line of Eq. (9), we have used the Fresnel coefficient identities  $t_{ij}t_{ji} - r_{ij}r_{ji} = 1$  and  $r_{ij} = -r_{ji}$  [13], and from that line we find that the condition  $\mathcal{R}_{1s} = 0$  is satisfied if

$$R_{per} = r_{a1}, \quad (10)$$

which we refer to as our *matching condition*. When considering the propagation of the LRSP, if the multilayer is to simulate a uniform substrate with dielectric constant equal to that of the cladding, or at least nearly so, this condition must be satisfied, or nearly satisfied, when the Fresnel coefficients are evaluated at  $\kappa_{res}^{sym}$ .

To establish a protocol for designing such a multilayer, it is useful to begin by neglecting all loss in the cladding and the metal, and any that might be present in the multilayer. In this approximation  $\varepsilon_1$  is replaced by its real part, and  $\kappa_{res}^{sym}$  and  $n_{eff}^{sym}$  are replaced by their real parts. This lossless approximation will allow us to winnow down the parameter space easily, to the point that the design can be completed; *thus until the last three paragraphs of this section we assume  $\kappa_{res}^{sym} = \tilde{\omega}n_{eff}^{sym}$  and  $\varepsilon_1$  to be real in our analyses, and use the real parts of the actual quantities in our calculations.*

Since  $n_{eff}^{sym} > n_1$  we immediately have  $|r_{a1}| = 1$ , indicating that the field is evanescent in the cladding, and thus from (10) we must have  $|R_{per}| = 1$ . If the dielectric constants of the layer materials are large enough so that the fields are propagating within the layers themselves ( $w_a$  and  $w_b$  real), this requires that at  $\kappa_{res}^{sym}$  we are within one of the photonic band gaps of the multilayer structure, so that the overall field structure is evanescent in the multilayer, and the reflectivity  $R_{per}$  is of unit norm. To identify the condition for this to be so, note that the unit cell transfer matrix of the periodic multilayer structure is  $m_{unit} = m_a(d_a)m_{ab}m_b(d_b)m_{ba}$ , with  $m_{ij}$  the interface transfer matrix between medium  $i$  and  $j$ , and  $m_i(d_i)$  the propagation transfer matrix in medium  $i$  [13];  $R_{per}$  is calculated from the eigenvector of  $m_{unit}$ ,

$$m_{unit} \begin{pmatrix} R_{per.} \\ 1 \end{pmatrix} = \lambda \begin{pmatrix} R_{per.} \\ 1 \end{pmatrix}, \quad (11)$$

with eigenvalue  $\lambda = e^{i\mu L}$ , where  $L = d_a + d_b$ , and  $\mu$  is the complex Bloch wavenumber. For an overall field structure that is evanescent in the multilayer structure, signalling that we are in a photonic band gap, we must have  $|\lambda| > 1$  [14]. Writing the unit cell matrix elements by  $A, B, C$ , and  $D$ ,

$$m_{unit} = \begin{pmatrix} A & B \\ C & D \end{pmatrix}, \quad (12)$$

we have

$$R_{per} = \frac{B}{\lambda - A}, \quad (13)$$

with

$$\lambda = \frac{A + D}{2} \pm \sqrt{\left(\frac{A + D}{2}\right)^2 - 1}. \quad (14)$$

[14]. The matrix elements of (12) are found by multiplying the transfer matrices of which it is composed; in particular we find

$$\frac{A + D}{2} = \frac{1}{1 - r_{ba}^2} (\cos(w_a d_a + w_b d_b) - r_{ba}^2 \cos(w_a d_a - w_b d_b)). \quad (15)$$

Location within a band gap ( $\mu$  purely imaginary,  $\lambda$  real) is thus signalled by  $|A + D|/2 > 1$ . At the band edges,  $\lambda = \pm 1$  and  $|A + D|/2 = 1$  [14]. It is within the band gaps that we have  $|R_{per.}| = 1$ , and it is there we must seek to satisfy Eq. (10).

We consider addressing this task once a choice of multilayer materials has been made, with  $\varepsilon_a$  and  $\varepsilon_b$  fixed. If we then consider letting  $d_a \rightarrow 0$ , any existing band gap will necessarily vanish, since the medium will become uniform, and at best we can have  $|A + D| = 2$  in the limit. From (15) we see that as  $d_a \rightarrow 0$  there are only discrete  $d_b$  where this will hold; only for these  $d_b$  does the band gap survive until  $d_a = 0$ . We can plot these as points  $(0, d_b)$  in the plane of points  $(d_a, d_b)$ . Similarly, as  $d_b \rightarrow 0$  there are only discrete  $d_a$  for which  $|A + D| = 2$ , signalling for which  $d_a$  the band gap will survive until  $d_b = 0$ . Connecting the corresponding discrete points  $(0, d_b)$  and  $(d_a, 0)$  in the  $(d_a, d_b)$  plane by straight lines should then give a rough indication of the location of the band gaps as  $d_a$  and  $d_b$  are varied. Those straight lines are easily found to be identified by

$$w_a d_a + w_b d_b = m\pi \quad \text{with} \quad m = 1, 2, 3, \dots \quad (16)$$

We illustrate this by considering periodic multilayers of  $\text{SiO}_2$  and  $\text{TiO}_2$ , taking the dielectric constants of  $\text{SiO}_2$  and  $\text{TiO}_2$  as  $\varepsilon_{\text{SiO}_2} = \varepsilon_a = 2.0932$  [9] and  $\varepsilon_{\text{TiO}_2} = \varepsilon_b = 7.421$  [15], respectively. In Fig. 2a we plot the solutions of Eq. (16) as dotted lines. The solid lines indicate the solutions for the band edges ( $|A + D| = 2$  for  $d_a$  and  $d_b$  in general both nonzero), with the region in between each pair of lines indicating the values of  $(d_a, d_b)$  for which there is a photonic bandgap. We see that the dotted lines do indeed give a good indication of where in the  $(d_a, d_b)$  plane the band gaps lie; we refer to the lines identified by Eq. (16) as *guide lines*. Note that the canonical ‘‘quarter-wave stack’’ with  $w_a d_a = w_b d_b = \pi/2$ , lies within the first band gap and in fact is precisely on the line (16) with  $m = 1$ .

To satisfy the matching condition (10) at  $\kappa_{sym}^{res}$  we must be in the band gap region ( $|R_{per.}| = |r_{a1}|$ ) and have  $\arg R_{per} = \arg r_{a1}$ . It is easy to determine where the latter condition is satisfied in the band gap region, and we plot that as the blue dash dotted line in Fig. 2b, together with the solutions of Eq. (16), again as dotted

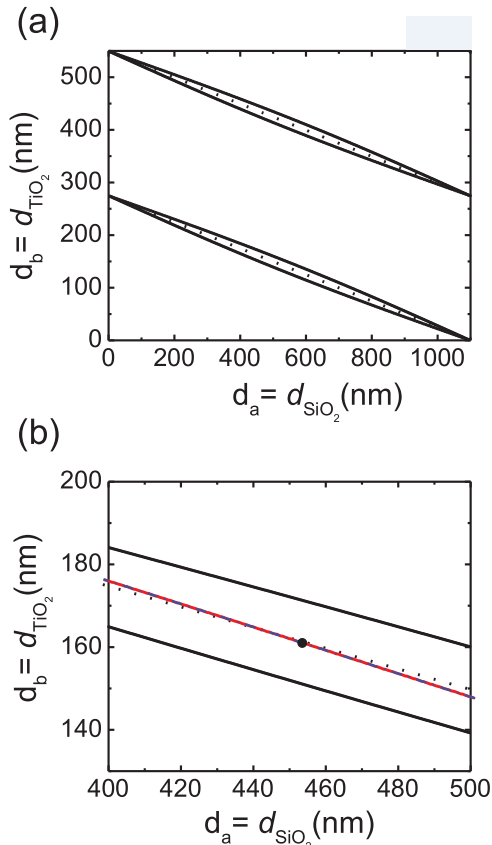


FIG. 2. (a) The  $d_{\text{SiO}_2}$  and  $d_{\text{TiO}_2}$  (solid black lines) for which  $\kappa_{\text{res}}^{\text{sym}}$  is on a bandedge of the periodic multilayer structure in the lossless case, and the straight lines of  $w_{\text{SiO}_2} d_{\text{SiO}_2} + w_{\text{TiO}_2} d_{\text{TiO}_2} = m\pi$  (black dotted lines), with  $m = 1, 2$ . (b) The  $d_{\text{SiO}_2}$  and  $d_{\text{TiO}_2}$  (blue dash-dotted line) for which  $\arg R_{\text{per}} = \arg r_{a1}$  is satisfied at  $\kappa_{\text{res}}^{\text{sym}}$ , when the losses are ignored, and the  $d_{\text{SiO}_2}$  and  $d_{\text{TiO}_2}$  (red solid line) for which  $R_{\text{per}} = r_{a1}$  is satisfied at a  $\kappa$  close to  $\kappa_{\text{res}}^{\text{sym}}$ , when the losses are considered. The large black dot indicates the choice of the parameters for the specific multilayer structure studied in the rest of this paper.

lines, where we focus on a region of the  $(d_a, d_b)$  plane where the  $m = 1$  guide line is close to the center of the band gap region. Thus in the lossless limit it is possible to choose a multilayer structure so that (10) is exactly satisfied, and the LRSPs in the symmetric and antisymmetric structures share the same  $\kappa_{\text{res}}^{\text{sym}}$ . We note that while the structures that do this are characterized by values  $(d_a, d_b)$  that lie close to the guide lines, the solutions of  $\arg R_{\text{per}} = \arg r_{a1}$  do not run all the way to  $d_a = 0$  and  $d_b = 0$ , as do the guide lines, for before those limits are reached the solutions encounter the band edges.

We now reinstate loss in  $\kappa_{\text{res}}^{\text{sym}}$  and in the water cladding. We no longer have  $|R_{\text{per}}| = |r_{a1}|$  automatically holding in the previously identified band gap regions

of the  $(d_a, d_b)$  plane, as we did in the absence of loss, and so to achieve (10) we would have to satisfy *two* non-trivial conditions,  $|R_{\text{per}}| = |r_{a1}|$  and  $\arg R_{\text{per}} = \arg r_{a1}$ . We can find curves in the  $(d_a, d_b)$  plane where each of these conditions is satisfied, but for our choice of materials these curves do not intersect. So at least for some choices of dielectric materials it is impossible to satisfy (10) at  $\kappa_{\text{res}}^{\text{sym}}$  in the ubiquitous presence of loss; we cannot simply replace a uniform substrate with a periodic multilayer structure and maintain the same LRSP.

Nonetheless, we can find complex values of  $\kappa$  close to  $\kappa_{\text{res}}^{\text{sym}}$  where (10) is satisfied. They can be identified by choosing thicknesses  $(d_a, d_b)$  close to one of the guide lines, and searching in the complex plane for values of  $\kappa$  that satisfy (10); we denote such solutions by  $\kappa_{\text{res}}^{\text{asym}}$ . In fact this is possible for a wide range of values  $(d_a, d_b)$ , indicated by the red lines in Fig. 2b. The guide lines provide a good indication of where the values  $(d_a, d_b)$  of interest should be sought, although as in the lossless limit solutions  $\kappa_{\text{res}}^{\text{asym}}$  cannot be found all the way to  $d_a = 0$  and  $d_b = 0$ . Note that in general the different points on the red line in Fig. 2b correspond to different values of  $\kappa_{\text{res}}^{\text{asym}}$ , unlike the different points on the blue dash-dotted line, which all correspond to solutions of Eq. (10) with the Fresnel coefficients evaluated at  $\text{Re}\kappa_{\text{res}}^{\text{sym}}$ .

A reasonable design strategy is to adopt thicknesses  $(d_a, d_b)$  associated with the center of the band gap region, resulting in an LRSP with a field in the multilayer well-confined near the metal, and for which we can expect a better tolerance for any fabrication errors. In line with this, but still somewhat arbitrarily, we take  $d_{\text{SiO}_2} = d_a = 453.5$  nm and  $d_{\text{TiO}_2} = d_b = 161$  nm for the rest of this paper. This yields an  $n_{\text{res}}^{\text{asym}} = \kappa_{\text{res}}^{\text{asym}}/\tilde{\omega} = 1.31824 + i5.17 \times 10^{-5}$ , corresponding to a loss of 2.15dB/mm and an energy propagation length of about 2mm. The real part of  $n_{\text{res}}^{\text{asym}}$  is very close to the real part of  $n_{\text{res}}^{\text{sym}}$ , and the loss for the asymmetric structure is actually slightly less than for the LRSP of the original symmetric structure. Thus while our original goal was to match  $\kappa_{\text{res}}^{\text{sym}}$  and achieve the low loss of a LRSP in a symmetric structure, we find that using a multilayer structure it is possible to achieve even lower loss than in a symmetric structure; we plan to return to this in future communications.

### III. SYMMETRIC AND ASYMMETRIC LRSP FIELDS

Some insight into the nature of the LRSPs in the infinite symmetric and asymmetric structures we have considered (see Fig. 3) can be gained by comparing the LRSP field profiles in the two structures. A fair comparison involves field profiles that are associated with the different structures and have the same field energy. Since loss is present, the field energy for a LRSP cannot be strictly defined, but since the loss is small in the sense that the LRSP can propagate many wavelengths before

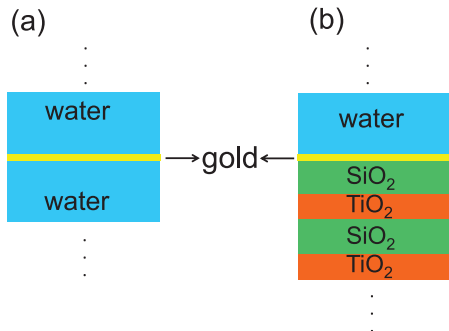


FIG. 3. (a) An infinite symmetric structure supporting LRSP, with a  $20\text{nm}$  gold layer. (b) An infinite asymmetric multilayer structure supporting LRSP, with a  $20\text{nm}$  gold layer, and a periodic multilayer structure of  $\text{SiO}_2$  and  $\text{TiO}_2$ , with  $d_{\text{SiO}_2} = 453.5\text{nm}$  and  $d_{\text{TiO}_2} = 161\text{nm}$ .

decaying, we can proceed by replacing the complex quantity  $1/\varepsilon(z, \omega)$ , where  $\varepsilon(z, \omega)$  is the position and frequency dependent dielectric constant, by  $\text{Re}(1/\varepsilon(z, \omega))$ , and using the standard expression for energy density in a dispersive medium to construct mode profiles corresponding to the same energy in both structures [16]. Scaling the electric field intensity (*i.e.*,  $|E|^2$ ) of the field profiles of the two structures in the same way yields the results shown in Fig. 4. The electric field intensity in the cladding ( $z > 0$ )

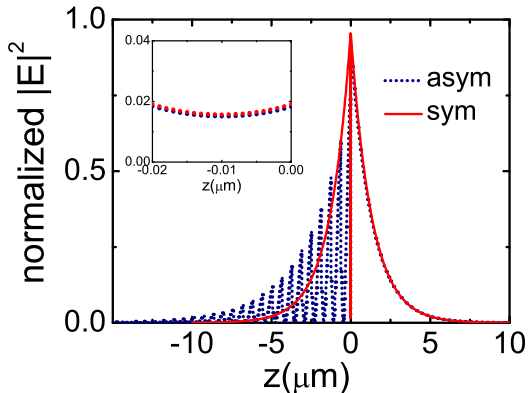


FIG. 4. The normalized electric field intensity profile (see text below) of the resonant mode of the asymmetric structure (dot blue line) and the LRSP mode of the symmetric structure (solid red line). Inset: the zoomed intensity profile in gold. The  $z$  axis is normal to the plane of the structure, and the (top) gold-water interface is at  $z = 0$ .

is evanescent, and almost the same in the two structures. In the metal layer (inset), the electric field intensity in the multilayer structure is similar to, and even slightly smaller than, the field intensity in the symmetric structure; it is for this reason that the loss of the mode in the asymmetric structure is slightly smaller than that of the

mode in the symmetric structure. While  $|E|^2$  is symmetric about the center of the gold film in the symmetric structure, it exhibits an evanescent envelope function in the multilayer in the asymmetric structure. However, due to the multiple reflections and interferences in the layers, there are oscillations in  $|E|^2$  indicative of the photonic band gap. Compared to an earlier proposed multilayer structure for the LRSP [11], in this structure the field is less confined, but is also much smaller in the metal layer, and therefore the absorption losses are smaller.

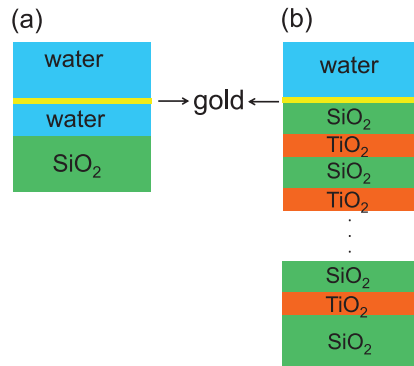


FIG. 5. (a) A finite symmetric (b) finite asymmetric multilayer structure, supporting LRSP.

In realistic structures the behaviour of the fields is modified by the presence of substrates. While we continue to treat the cladding as infinite, assuming that in sensing applications the thickness of the water above the gold will be greater than the evanescent decay length of the field, we now consider the gold to be deposited on a finite multilayer structure with an  $\text{SiO}_2$  substrate (see Fig. 5b). For comparison we also consider a structure with an  $\text{SiO}_2$  substrate placed a finite distance below the gold film in an otherwise symmetric structure (see Fig. 5a). The properties of the LRSP that result in these structures can be studied by considering coupling into them with an incident field from the substrate, which is the usual Kretschmann configuration [17]. In such an excitation the field inside the cladding is typically maximized when the rate of energy absorption in the metal layer equals the rate of energy incident from the substrate, and thus this usually identifies an optimum structure for sensing applications. Although this design target can be identified by pole analysis strategies [18], it can also be found simply by examining a series of reflectivity calculations for different thicknesses. For the symmetric structure we find that this critical coupling occurs when the thickness of the water layer below the gold film is about  $4.59\mu\text{m}$ , and for the asymmetric structure we find that it occurs when the number of periods is 25, leading to a multilayer thickness of  $15.36\mu\text{m}$ .

In Fig. 6a we plot the reflectivity  $|\mathcal{R}|^2$  of the two structures, each at its critical coupling thickness, as a function of incident angle;  $\mathcal{R}$  is the Fresnel coefficient

for  $p$ -polarized light incident from the substrate. The enhancement of the fields at the surface of each structure is determined by the Fresnel transmission coefficient from the substrate to the cladding for  $p$ -polarized light,  $\mathcal{T}$ , and we see from Fig. 6b that enhancements in the square of the field of the order of 400 is expected. The narrow resonances shown in these plots indicate poles in the Fresnel coefficients  $\mathcal{R}$  and  $\mathcal{T}$ . With respect to the poles in the corresponding infinite structures (see Fig. 3), the real parts of the poles are shifted slightly and the imaginary parts increased (and thus the loss increased) due to radiative coupling into the substrate. A search in the complex plane finds the pole for the symmetric structure at  $\kappa = \tilde{\omega}n_{eff}^{sym}$ , where  $n_{eff}^{sym} = 1.31814 + i1.106 \times 10^{-4}$ , with the imaginary part corresponding to a loss of about 4.6dB/mm, or equivalently an energy propagation length of about 0.94mm, and the pole for the asymmetric structure at  $\kappa = \tilde{\omega}n_{eff}^{asym}$ , where  $n_{eff}^{asym} = 1.31825 + i1.053 \times 10^{-4}$ , with the imaginary part corresponding to a loss of about 4.39dB/mm, or equivalently an energy propagation length of 1mm.

The dips in the reflectivities in Fig. 6a occur at angles  $\theta^{sym,asym}$  associated with the real part of effective indices,  $\text{Re}n_{eff}^{sym} = n_{SiO_2} \sin\theta^{sym}$  and  $\text{Re}n_{eff}^{asym} = n_{SiO_2} \sin\theta^{asym}$  respectively, where  $n_{SiO_2} = 1.447$  is the index of refraction of the substrate at  $\lambda = 1310\text{nm}$ , and the widths of the dips are associated with the imaginary parts of the effective indices. We note that the poles of the Fresnel coefficients extracted from equations such as Eq. (4) are used to approximate the values of Fresnel coefficients by pole expansions valid for real  $\kappa$ , which are the appropriate  $\kappa$  for excitation in a Kretschmann configuration as discussed here, or for use in superpositions to describe pulse propagation along a structure [19]. Thus in extracting these poles we should choose a definition of the square roots of  $w_i(\kappa)$  such that the calculated values of the Fresnel coefficients in the upper half of the complex  $\kappa$  plane join continuously to those calculated on the real  $\kappa$  axis. Here this can be guaranteed by choosing a branch cut that lies along the negative imaginary  $\kappa$  axis.

If we turn from Kretschmann configurations to applications involving end-fire coupling into LRSPs, optimization for sensing applications typically involves the minimization of propagation loss. That loss decreases as the thickness of the structure between the metal film and the substrate increases, for as increasing thickness the radiative loss of light into the substrate becomes less and less. In Fig. 7 the calculated losses of the LRSPs in the symmetric and asymmetric structures are shown as a function of the thickness of the structure, as extracted from the poles of the Fresnel coefficients. In the symmetric structure, for a water layer thickness larger than about  $15\mu\text{m}$  the mode loss approaches a limiting value of 2.23dB/mm, corresponding to the mode loss of the infinite structure; in the asymmetric structure, for a multilayer thickness larger than about  $30\mu\text{m}$  (49 periods), the mode loss approaches a limiting value of 2.15dB/mm, corresponding

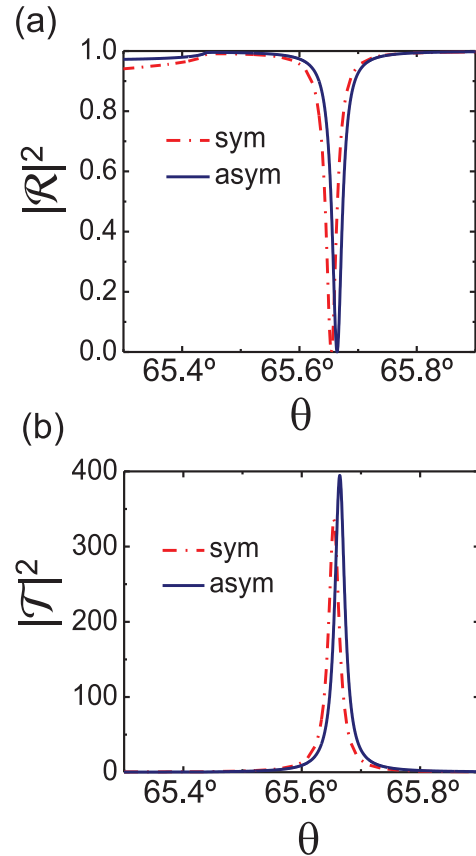


FIG. 6. (a) Reflectivity  $|\mathcal{R}|^2$ , and (b) enhancement factor of the square of the field  $|\mathcal{T}|^2$  (see text) for the symmetric (red dash dotted line) and the asymmetric (blue solid line) structures, both as a function of the angle of incidence from the substrate.

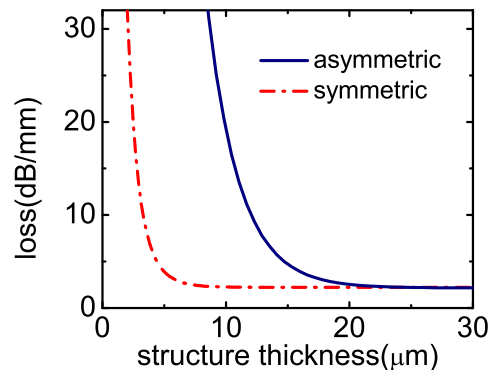


FIG. 7. The loss of the LRSP in the symmetric (dash dot red line) and asymmetric (solid blue line) structures, as the thickness of the structures changes.

to the mode loss of the infinite structure.

#### IV. SENSING WITH PLANAR RESONANT STRUCTURES

Resonant structures supporting guided modes, such as those considered above, have their optical properties modified by the presence of new species on or near the surface of the structure. This can lead to their application as sensors, for the new species are located precisely where the optical fields are largest, and thus their effect on the properties of the guided modes can be significant. In this section we derive a semi-analytic expression for a standard surface sensing parameter that characterizes the effectiveness of such a sensor, and apply it to the structures we have introduced in the last section.

We begin generally and consider an arbitrary planar resonant structure (Fig. 8a), supporting a resonant mode at a complex wavenumber  $\kappa_{res}^0 = \kappa_R + i\kappa_I$ . If a thin molecular layer with effective dielectric constant  $\varepsilon_2$  is placed on the structure (Fig. 8b), the complex wavenumber of the mode shifts, and a surface sensing parameter can be defined [4] as

$$G = \frac{1}{\kappa_I} \frac{\partial}{\partial d} \text{Re}(\Delta\kappa_{res}), \quad (17)$$

where  $\Delta\kappa_{res} = \kappa_{res}^m - \kappa_{res}^0$ , and  $\kappa_{res}^m$  is the complex wavenumber of the mode in the presence of the molecular layer. For  $\kappa$  close to  $\kappa_{res}^0$  we can use a pole expansion

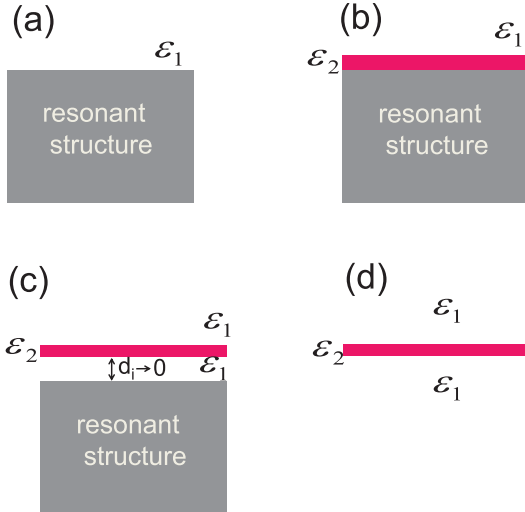


FIG. 8. (a) A bare resonant structure, with a cladding of dielectric constant  $\varepsilon_1$ , (b) with a thin layer of molecules with dielectric constant  $\varepsilon_2$  on top, (c) an infinitesimally thin layer of medium 1 under the molecular layer, and (d) the molecular layer between two media with dielectric constant  $\varepsilon_1$ .

[19, 20] for the reflection coefficient from the cladding to

the bare resonant structure, which we now denote very generally by  $\bar{R}_{1s}$ , such that

$$\bar{R}_{1s} \simeq \frac{\rho_{1s}}{\kappa - \kappa_{res}^0}, \quad (18)$$

where  $\rho_{1s}$  characterizes the pole strength and is in general complex. For the resonant structure with the molecular layer on top, modelled as a thin dielectric film, we can construct an expression for the Fresnel reflection coefficient  $\bar{R}'_{1s}$  in terms of  $\bar{R}_{1s}$  by adding an infinitesimally thin layer, with a thickness  $d_i \rightarrow 0$  and a dielectric constant  $\varepsilon_1$ , just below the molecular layer (Fig. 8c). Then

$$\bar{R}'_{1s} = R + \frac{T\bar{R}_{1s}T}{1 - R\bar{R}_{1s}}, \quad (19)$$

where  $R$  and  $T$  are the Fresnel reflection and transmission coefficients for the molecular layer sandwiched between two media with dielectric constant  $\varepsilon_1$  (Fig. 8d). Inserting Eq. (18) in Eq. (19),

$$\bar{R}'_{1s} = R + \frac{T\rho_{1s}T}{\kappa - (\kappa_{res}^0 + R\rho_{1s})}, \quad (20)$$

implying that the complex wavenumber of the mode in the presence of molecules,  $\kappa_{res}^m$ , is  $\kappa_{res}^m = \kappa_{res}^0 + R\rho_{1s}$ , and the shift in the complex wavenumber is

$$\Delta\kappa_{res} = R\rho_{1s}. \quad (21)$$

The pole strength  $\rho_{1s}$  is a parameter of the bare resonant structure, and does not depend on the properties of the molecular layer; in general it must be determined numerically. The reflection coefficient  $R$  (see Fig. 8d), however, is

$$R = r_{12} + \frac{t_{12}r_{21}t_{21}e^{2iw_2d}}{1 - r_{21}r_{21}e^{2iw_2d}}, \quad (22)$$

where  $d$  is the thickness of the molecular layer, and  $r_{12}$ ,  $t_{12}$ ,  $r_{21}$ , and  $t_{21}$  are the Fresnel reflection and transmission coefficients between the cladding and the molecular layer (recall (2),(3)). Inserting Eq. (2) or (3) into Eq. (22), for thin molecular layers, where

$$(w_1 \pm w_2)d \ll 1, \quad (23)$$

for  $s$ -polarization we find

$$R \simeq \frac{n_{os}}{1 - n_{os}}, \quad (24)$$

with

$$n_{os} = \frac{i\tilde{\omega}^2}{2w_1}(\varepsilon_2 - \varepsilon_1)d,$$

while for  $p$ -polarization

$$R \simeq \frac{n_-}{1 - n_+}, \quad (25)$$

where

$$n_{\pm} = \frac{i\kappa^2 (\varepsilon_2 - \varepsilon_1)d}{2w_1 \varepsilon_2} \pm \frac{iw_1 (\varepsilon_2 - \varepsilon_1)d}{2 \varepsilon_1}.$$

These calculations agree with the similar calculations presented earlier by Cheng et al. [21]; using Eq. (24) or (25), and (21) in Eq. (17), we find a semi-analytic expression for the surface sensing parameter in terms of the thickness of the molecular layer, the dielectric constants of the molecular layer and the cladding, and the pole strength. We assume a molecular layer with an effective index of refraction of 1.5 and thickness up to  $10nm$ , and calculate the sensing parameters for the symmetric and asymmetric structures discussed in the previous section, both exactly by numerically determining the shift  $\Delta\kappa_{res}$  in the position of the pole of the full structures, and approximately from the semi-analytic expressions presented in this section; here the  $p$ -polarized expressions are the relevant ones. In Fig. 9 we show the results for  $\text{Re}(\Delta\kappa_{res})/\kappa_I$  of the infinite symmetric and asymmetric structures. The semi-analytic calculations match with the exact calculations for  $d < 5nm$ , but as the thickness of the molecular layer increases the assumption (23) loses its validity and the approximated calculations deviate more from the exact calculations; nonetheless, they remain accurate to about 10% for thicknesses as large as  $10nm$ . The slope of the curves in Fig. 9 around  $d = 0$  gives  $G$ , and we find  $G = 1.09nm^{-1}$  and  $G = 1.28nm^{-1}$  for the infinite symmetric and asymmetric structure, respectively; the larger  $G$  for the asymmetric structure is due to the slightly smaller resonance width ( $\kappa_I$ ) in the asymmetric structure. From Fig. 7, it is clear that if the thickness of the finite symmetric (or asymmetric) structure is larger than about  $15\mu m$  (or  $30\mu m$ ), the loss in the structure is about the loss in the corresponding infinite structure. As expected, the results for  $\text{Re}(\Delta\kappa_{res})/\kappa_I$  for a  $15\mu m$  symmetric structure and a  $30\mu m$  asymmetric structure are indistinguishable from the corresponding infinite structures, as shown in Fig. 9. We have done similar calculations for the finite symmetric and asymmetric structures at thicknesses corresponding to the critical coupling thickness ( $4.590\mu m$  for the symmetric structure and  $15.362\mu m$  for the asymmetric structure), and the result is shown in Fig. 10. These would be relevant for sensing in a Kretschmann configuration rather than an end-fire coupling configuration. We find  $G = 0.55nm^{-1}$  and  $G = 0.63nm^{-1}$  for the finite symmetric and asymmetric structures, respectively, which are smaller than the corresponding values shown in Fig. 10, as the coupling losses are larger here.

## V. CONCLUSION

In this paper we have presented a new strategy for designing asymmetric multilayer structures that support LRSPs. We have shown that if the Fresnel reflection coefficient from the cladding to the multilayer structure be-

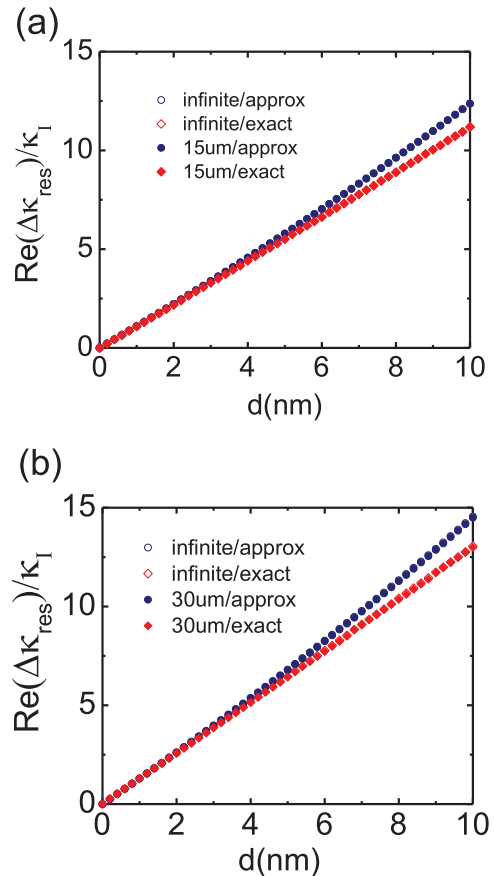


FIG. 9. The shift in the resonance wavenumber divided by the width of the resonance for the (a) infinite and  $15\mu m$  symmetric and (b) infinite and  $30\mu m$  asymmetric structures. The circles and the diamonds are the semi-analytic and exact calculations, respectively. The hollow circles and diamonds correspond to the infinite structures calculations, and overlap with the full circles and diamonds that correspond to the finite structures calculations.

low the metal film vanishes at the complex wavenumber of the LRSP in a symmetric structure, the LRSP resonance condition for the symmetric and asymmetric multilayer structures become the same, and the asymmetric structure supports a LRSP equivalent to that supported in the symmetric structure. For an arbitrary choice of materials for the multilayer structure it is impossible to satisfy this condition exactly, but at complex wavenumbers close to that of the LRSP in the symmetric structure a resonance condition can be found, in some instances with even less loss than that of the LRSP in the symmetric structure.

We have provided a protocol for determining this resonance condition based on first describing a model system without loss, and then including the loss in the final design. We have also studied how the losses depend on the



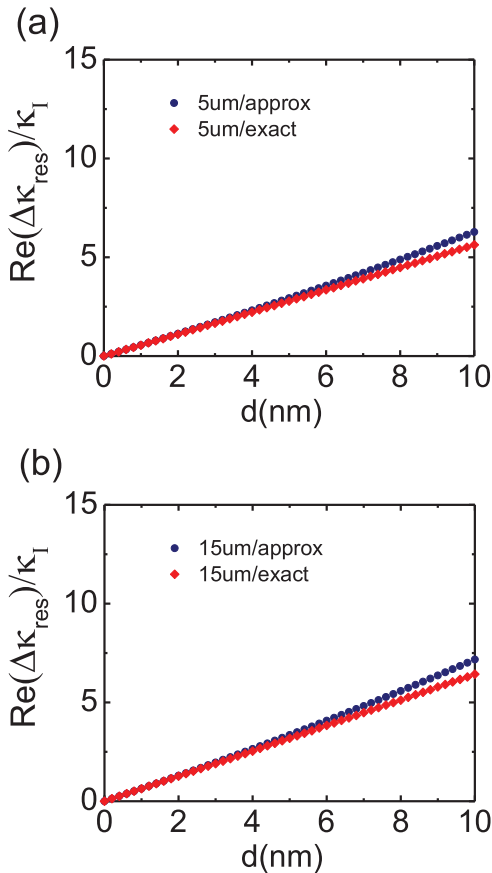


FIG. 10. The shift in the resonance wavenumber divided by the width of the resonance for the (a)  $4.590\mu\text{m}$  symmetric and (b)  $15.362\mu\text{m}$  asymmetric structures. The circles and the diamonds are the semi-analytic and exact calculations, respectively.

thickness of the multilayer structure, taking into account radiative contributions to the substrate. For a multilayer of  $\text{SiO}_2$  and  $\text{TiO}_2$  we have found that the radiative losses are negligible if the multilayer structure thickness is about or greater than  $30\mu\text{m}$ . For biosensing applications involving an arbitrary planar resonant structure, we have derived a semi-analytic expression for a standard surface sensing parameter identifying the dependence of the sensing parameter on the dielectric constant of the molecular layer, its thickness, and the original pole strength of the resonance on the bare structure; for typical parameters

we find that there is a good match between these semi-analytic expressions and the exact results if the thickness of the molecular layer is less than about  $5\text{nm}$ , with corrections only on the order of about 10% for molecular layer thicknesses up to  $10\text{nm}$ . For a  $20\text{nm}$  gold film the surface sensing parameter for the  $30\mu\text{m}$  thick multilayer structure is  $G = 1.28\text{nm}^{-1}$ , larger than the value of  $G = 1.09\text{nm}^{-1}$  for a  $15\mu\text{m}$  thick symmetric structure.

Compared to the  $20\text{nm}$  gold structure of Min et al. [9], which has an intensity attenuation of  $3.26\text{dB/mm}$  and a surface sensing parameter  $G = 1.29\text{nm}^{-1}$ , our asymmetric multilayer structure has a smaller loss (minimum of  $2.15\text{dB/mm}$ ) and a similar sensing parameter ( $G = 1.28\text{nm}^{-1}$ ). However, the structure of Min et al. [9] is a thin film suspended in air, and compared to our multilayer structure is expected to be less stable and harder to fabricate. Compared to the multilayer structure studied by Konopsky et al. [11], the multilayer structure we present here is fully periodic, and does not require an additional layer between the metal and the periodic multilayer. However, a direct comparison of the losses and the surface sensing parameters of these two structures is not possible, as the metal layer in the work of Konopsky et al. [11] is palladium, which is lossier than gold. Nevertheless, if the number of the periods in that multilayer structure is increased from 14 periods, the mode losses can be decreased by a factor of two. More generally, the design strategy presented here can be applied to a range of structures involving other metals and other multilayers to systematically explore the parameter space and optimize the predicted behavior.

In previous work [20], we calculated Raman scattering from molecules on planar resonant dielectric structures, and showed that the Raman signal is enhanced when the pump field couples to a resonant mode. The asymmetric multilayer structure we studied in this paper can also be used as a substrate for surface enhanced Raman scattering (SERS) [22], when the pump field is coupled to the LRSP excitation. In particular, we expect that the good surface functionalization of gold films may make these structures more promising SERS substrates than fully dielectric multilayer structures [23].

## VI. ACKNOWLEDGEMENTS

This work was supported by BiopSys: the Natural Sciences and Engineering Research Council of Canada Strategic Network for Bioplasmonic Systems.

- 
- [1] H. Raether, *Surface Plasmons on Smooth and Rough Surfaces and on Gratings* (Springer, 1988).  
 [2] W. L. Barnes, A. Dereux, and T. W. Ebbesen, "Surface plasmon subwavelength optics," *Nature* **424**, 824-

830 (2003).

- [3] J. Homola, S. S. Yee, and G. Gauglitz, "Surface plasmon resonance sensors: review," *Sens. Actuators B Chem.* **54**, 3-15 (1999).

- [4] P. Berini, "Bulk and surface sensitivities of surface plasmon waveguides," *New Journal of Physics* **10**, 105010(1)-105010(37) (2008).
- [5] D. Sarid, "Long-Range Surface-Plasma Waves on Very Thin Metal Films," *Phys. Rev. Lett.* **47**, 1927-1930 (1981).
- [6] J. J. Burke, G. I. Stegeman, and T. Tamir, "Surface-polariton-like waves guided by thin, lossy metal films," *Phys. Rev. B* **33**, 5186-5201 (1986).
- [7] A. W. Wark, H. J. Lee, and R. M. Corn, "Long-range surface plasmon resonance imaging for bioaffinity sensors," *Anal. Chem.* **77**, 3904-3907 (2005).
- [8] R. Slavik, and J. Homola, "Ultra-high resolution long range surface plasmon-based sensor," *Sens. Actuators B Chem.* **123**, 10-12 (2007).
- [9] Q. Min, C. Chen, P. Berini, R. Gordon, "Long range surface plasmons on asymmetric suspended thin film structures for biosensing applications," *Optics Express* **18**, 19009-19019 (2010).
- [10] V. N. Konopsky and E. V. Alieva, "Long-Range Propagation of Plasmon Polaritons in a Thin Metal Film on a One-Dimensional Photonic Crystal Surface," *Phys. Rev. Lett.* **97**, 253904(1)-253904(4) (2006).
- [11] V. N. Konopsky and E. V. Alieva, "Long-range plasmons in lossy metal films on photonic crystal surfaces," *Optics Express* **34**, 479-481 (2009).
- [12] For details of the notation used here for Fresnel coefficients, see [13].
- [13] J. E. Sipe, "New Green function formalism for surface optics," *J. Opt. Soc. Am. B* **4**, 481-489 (1987).
- [14] A. Yariv and P. Yeh, *Optical Waves in Crystals* (Wiley, 2003).
- [15] <http://refractiveindex.info/>.
- [16] N. A. R. Bhat and J. E. Sipe, "Hamiltonian treatment of the electromagnetic field in dispersive and absorptive structured media," *Phys. Rev. A* **73**, 063808(1)-063808(25) (2006).
- [17] E. Kretschmann and H. Raether, "Radiative decay of nonradiative surface plasmons excited by light," *Z. Naturforsch. A* **23**, 2135-2136 (1968).
- [18] J.E. Sipe, unpublished.
- [19] J. E. Sipe and J. Becher, "Surface energy transfer enhanced by optical cavity excitation: a pole analysis," *J. Opt. Soc. Am. A* **72**, 288-295 (1982).
- [20] A. Delfan, M. Liscidini, and J. E. Sipe, "Surface enhanced Raman scattering in the presence of multilayer dielectric structures," *J. Opt. Soc. Am. B* **29**, 1863-1874 (2012).
- [21] T. Cheng, C. Rangan, and J. E. Sipe, "Metallic nanoparticles on waveguide structures: effects on waveguide mode properties and the promise of sensing applications," *J. Opt. Soc. Am. B* **30**, 743-765 (2013).
- [22] E. L. Ru and P. Etchegoin, *Principles of Surface-Enhanced Raman Spectroscopy: and related plasmonic effects* (Elsevier Science, 2008).
- [23] S. Pirodda, X.Xu, A. Delfan, S. Mysore, S. Maiti, G. Dacarro, M. Patrini, M.Galli, G. Guizzetti, D. Bajoni, J.E. Sipe, G. Walker, and M. Liscidini, "Surface enhanced Raman Scattering in purely dielectric structures via Bloch Surface Waves," *J. Phys. Chem.* **117**, 6821-6825 (2013).